

Design and Structural Characterization of Potent and Selective Inhibitors of Phosphatidylinositol 4 Kinase III β

Florentine U. Rutaganira,^{†,‡} Melissa L. Fowler,^{‡,‡} Jacob A. McPhail,[‡] Michael A. Gelman,^{§,‡} Khanh Nguyen,[§] Anming Xiong,[§] Gillian L. Dornan,[‡] Brandon Tavshanjian,[†] Jeffrey S. Glenn,^{§,||} Kevan M. Shokat,^{*,†} and John E. Burke^{*,‡}

[†]Howard Hughes Medical Institute and Department of Cellular and Molecular Pharmacology, University of California, San Francisco (UCSF), San Francisco, California 94143, United States

[‡]Department of Biochemistry and Microbiology, University of Victoria, Victoria, BC V8W 2Y2, Canada

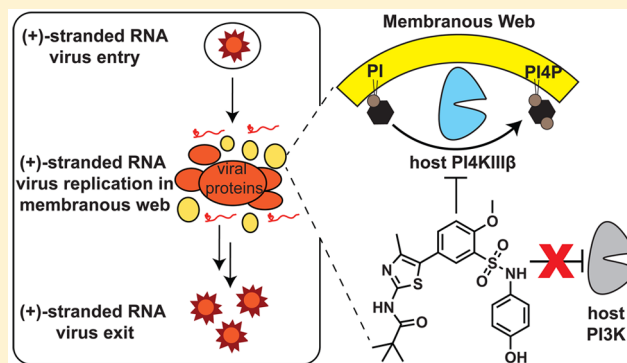
[§]Department of Medicine and Department of Microbiology & Immunology, Stanford University, Palo Alto, California 94305, United States

^{||}Veterans Administration Medical Center, Palo Alto, California 94304, United States

S Supporting Information

ABSTRACT: Type III phosphatidylinositol 4-kinase (PI4KIII β) is an essential enzyme in mediating membrane trafficking and is implicated in a variety of pathogenic processes. It is a key host factor mediating replication of RNA viruses. The design of potent and specific inhibitors of this enzyme will be essential to define its cellular roles and may lead to novel antiviral therapeutics. We previously reported the PI4K inhibitor PIK93, and this compound has defined key functions of PI4KIII β . However, this compound showed high cross reactivity with class I and III PI3Ks. Using structure-based drug design, we have designed novel potent and selective (>1000-fold over class I and class III PI3Ks) PI4KIII β inhibitors. These compounds showed antiviral activity against hepatitis C virus.

The co-crystal structure of PI4KIII β bound to one of the most potent compounds reveals the molecular basis of specificity. This work will be vital in the design of novel PI4KIII β inhibitors, which may play significant roles as antiviral therapeutics.



INTRODUCTION

Lipid phosphoinositides are essential regulators of myriad cellular processes, including signaling, membrane trafficking, and cytokinesis.¹ Phosphoinositides are generated through the phosphorylation of the inositol ring of phosphatidylinositol. Phosphatidylinositol can be phosphorylated and dephosphorylated by a diverse set of enzymes, and this results in a total of seven different mono- and polyphosphorylated phosphoinositides. The lipid species phosphatidylinositol 4-phosphate (PI4P) is generated by the action of phosphatidylinositol 4 kinases (PI4Ks).² PI4P is the main biosynthetic route for the multiply phosphorylated signaling lipids phosphatidylinositol 4,5-bisphosphate (PIP₂) and phosphatidylinositol 3,4,5-trisphosphate (PIP₃).³ In mammals, there are four different PI4K enzymes: two type II enzymes (PI4KII α and PI4KII β) and two type III enzymes (PI4KIII α and PI4KIII β). PI4KIII β is a peripheral membrane protein that is primarily localized at the Golgi and the trans-Golgi network (TGN). This enzyme plays key roles in mediating lipid transport⁴ and cytokinesis,⁵ maintaining lysosomal identity,⁶ and, in tandem with Rab GTPases, regulating membrane trafficking.⁷ Interest in the development of potent small molecules of PI4KIII β has been driven recently

by the discovery of the key role of this enzyme in mediating both viral replication⁸ and *Plasmodium* development.⁹

PI4KIII β is critical for mediating viral replication of a number of RNA viruses through the generation of PI4P-enriched viral replication platforms. These membranous webs enriched in PI4P play essential roles in spatially concentrating viral replication proteins and are key in intracellular viral replication. This process is essential for many human pathogenic viruses including poliovirus, coxsackieviruses, enterovirus 71, rhinovirus, and Aichi virus.^{8,10–14} There is also evidence that PI4KIII β together with PI4KIII α plays a key role in mediating viral replication of hepatitis C virus.¹⁴

Small molecule inhibitors of PI4KIII β are potent antiviral agents.^{8,15,16} We previously reported the potent PI4KIII β inhibitor PIK93 (compound 1),¹⁷ and this compound has been used extensively to decipher the cellular roles of PI4KIII β ^{4,18} and its role in mediating viral replication of pathogenic RNA viruses.^{8,11–14} Compound 1 potently inhibits PI4KIII β ; however, it shows cross reactivity toward a number of other lipid kinases.

Received: August 24, 2015

Published: February 17, 2016

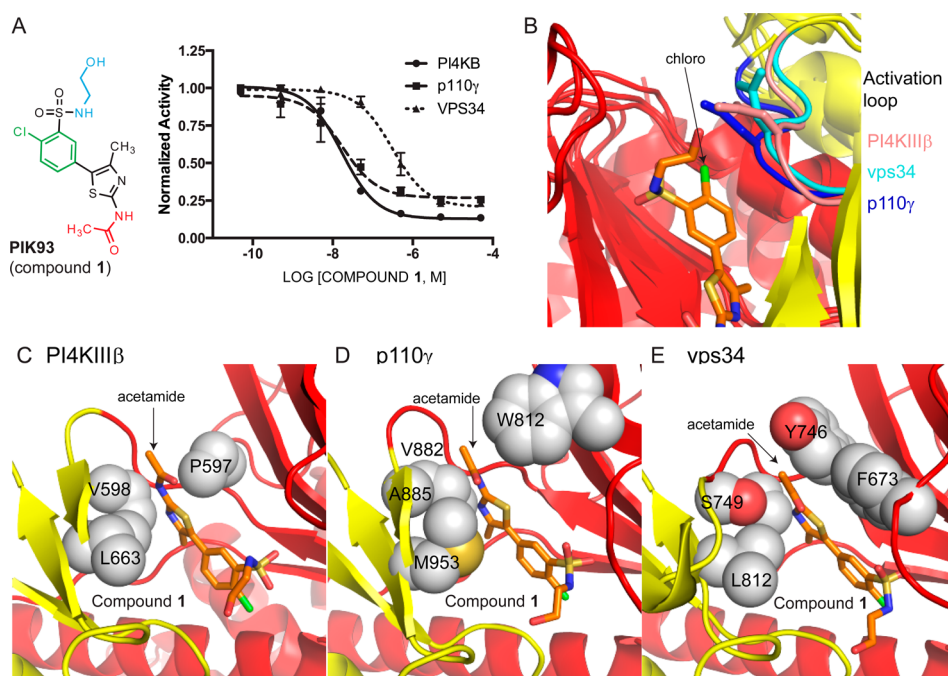


Figure 1. Structural basis for inhibition of PI4KIII β and PI3Ks by the inhibitor PIK93 (compound 1). (A) Structure of compound 1, with the ethanolamine substituent off of the sulfonamide colored blue, the chloro substituent off of the central phenyl colored green, and the acetamide substituent off of the thiazole colored red. The potency of 1 against PI4KIII β , PI3K γ , and vps34 is graphed. (B) Structures of PI4KIII β ¹⁹ (PDB ID: 4D0L), vps34²⁰ (PDB ID: 2X6J), and PI3K γ ¹⁷ (PDB ID: 2CHZ) bound to 1 aligned, showing the chloro substituent of 1 with the activation loop of each enzyme colored according to the legend. (C–E) Structures of PI4KIII β (C), PI3K γ (D), and vps34 (E) with residues within 5 Å of the acetamide group of 1 shown as spheres.

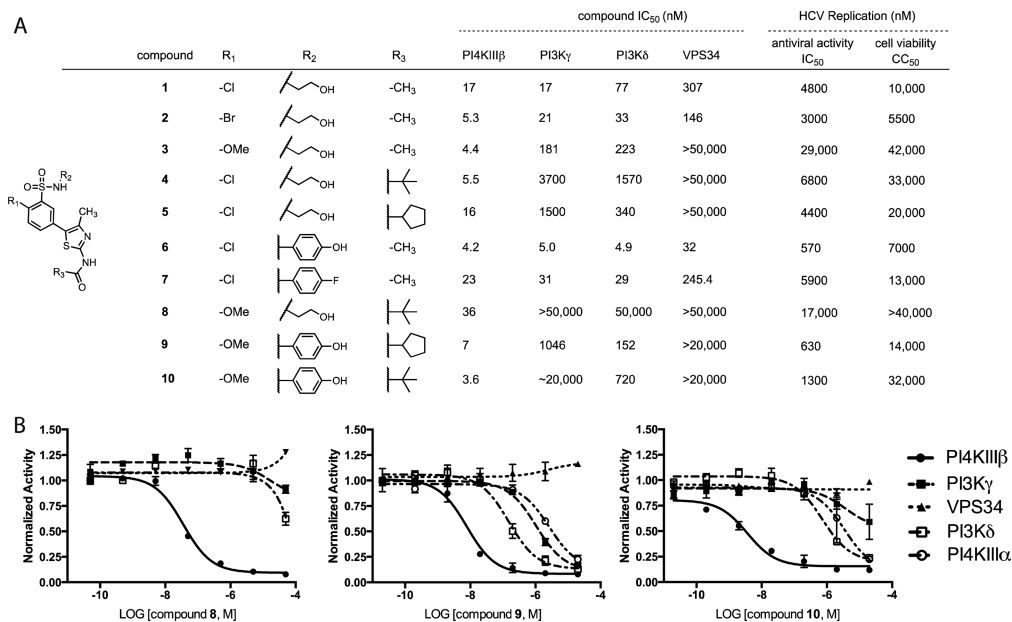


Figure 2. Development of novel PI4KIII β inhibitors. (A) Structure of compound 1 is shown, with novel substituents at the R₁, R₂, and R₃ positions shown in tabular form and with the IC₅₀ values for each compound against PI4KIII β , PI3K γ , PI3K δ , and vps34 listed. Kinase assays were carried out in the presence of 10 μ M ATP and 10 mM MgCl₂ (PI4KIII β , PI3K δ , and PI3K γ) or 10 mM MnCl₂ (vps34). IC₅₀ values measured using MnCl₂ are 10–20-fold higher than those with the physiologically relevant MgCl₂ due to increased kinase activity. Inhibitors anti-HCV antiviral activity (IC₅₀) was assessed by *Gaussia* luciferase assay (Gluc HCV2a activity), and cell viability (CC₅₀) was assessed by Presto Blue assay (Gluc HCV2a viability), as described in the Experimental Section. (B) Full inhibitor curves for compound 8–10 are shown for PI4KIII β , PI3K γ , PI3K δ , and vps34, with all measurements carried out in triplicate. For compounds 9 and 10, the curves for the related lipid kinase PI4KIII α is shown as well, with assays against other related lipid kinases shown in Figure S1.

Compound 1 has very similar IC₅₀ values for PI4KIII β , class III PI3 kinase (vps34), and class IB PI3K γ (Figure 1A). We have

previously crystallized 1 in complex with PI4KIII β ,¹⁹ vps34,²⁰ and PI3K γ ¹⁷ (Figure 1B–E).

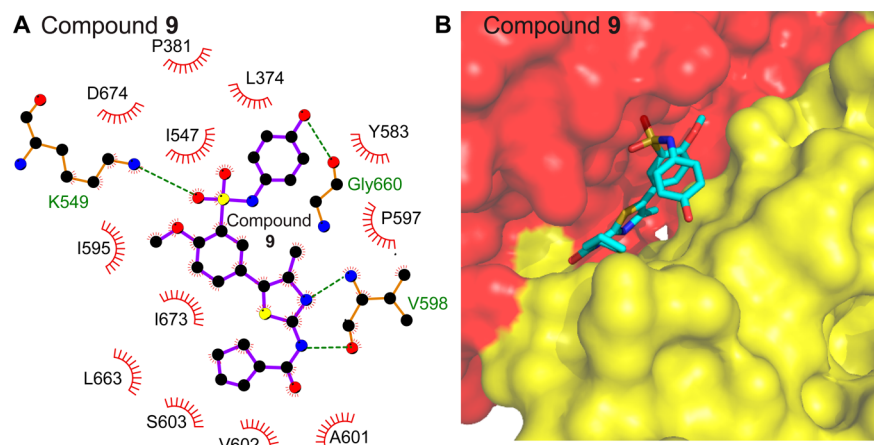


Figure 3. Structural basis of inhibition of PI4KIII β by compound 9. (A) Residues mediating the interaction of PI4KIII β with compound 9 are shown, with putative hydrogen bonds indicated by dotted lines. Figure generated using LIGPLOT.⁴³ (B) Fit of compound 9 in the PI4KIII β active site pocket. The kinase domain is colored with the N-lobe shown in red and the C-lobe shown in yellow.

Development of PI4KIII β as an effective drug target for antiviral therapeutics requires the generation of highly potent and specific inhibitors. We report the development of a set of derivatives from compound 1, and these represent some of the most potent PI4KIII β inhibitors reported to date. The selectivity profile of these compounds has been determined against vps34, PI3K δ , and PI3K γ , with the most selective compounds being >1000-fold selective over the related PI3K family of lipid kinases. We have successfully determined the structure of PI4KIII β bound to one of the most potent and selective compounds, and this structure reveals the molecular basis for the increased selectivity and potency of these compounds.

RESULTS

Design of Optimized PI4KIII β Inhibitors. Compound 1 is highly selective for PI4KIII β over PI4KIII α ; however, it is similarly potent for a number of phosphoinositide 3-kinases (PI3Ks), specifically the class I isoforms PI3K γ (also referred to as p110 γ) and PI3K δ (also referred to as p110 δ), as well as the class III PI3K vps34 (Figure 1A). The structures of 1 bound to vps34,²⁰ PI3K γ ,¹⁷ and PI4KIII β ¹⁹ revealed that within the binding pocket there were significant opportunities to modify 1 to increase both potency and selectivity for PI4KIII β .

From examining the structures of 1 bound to each enzyme, there were three regions of the molecule that were the focus to optimize both potency and selectivity of novel PI4KIII β inhibitors. These consisted of modifying the substituent on the central phenyl ring (colored green, Figure 1A), the substituent off of the sulfonamide (colored blue, Figure 1A), and the acetamide moiety (colored red, Figure 1A). The chloro substituent on the central phenyl ring of 1 fits into a pocket partially composed of the activation loop of both PI3Ks and PI4KIII β (Figure 1C). The conformation of the activation loop of PI3K γ when bound to compound 1 is positioned closer to this substituent than it is in either vps34 or PI4KIII β . This suggested that modifying this group to a larger substituent might increase selectivity over class I PI3Ks. Changing this group to a bromo substituent (compound 2) caused a slight increase in potency for PI4KIII β , PI3K δ , and vps34 and a slight decrease in potency for PI3K γ . Modifying this group to a methoxy substituent (compound 3) caused both an increase in potency for PI4KIII β and a large increase in specificity over PI3K γ , PI3K δ (>40-fold selective for both), and vps34 (Figure 2A).

The structures of 1 bound to PI4KIII β , PI3K γ , and vps34 also suggested that modification of the acetamide group derived from the central thiazole might lead to further gains in specificity. PI4KIII β has a much more open pocket around the acetamide group of 1 (Figure 1C) compared to that of both PI3K γ (Figure 1D) and vps34 (Figure 1E), which have a number of bulky hydrophobic residues. The methyl group of 1 was replaced with either a *t*-butyl group (compound 4) or a cyclopentyl group (compound 5). Both compounds showed similar or slightly better potency against PI4KIII β ; however, both showed a very large increase in selectivity over PI3K γ (>600-fold for compound 4 and >90-fold for compound 5), PI3K δ , and vps34 (Figure 2A).

Finally, the ethanolamine attached to the sulfonamide in compound 1 was also derivatized. The ethanolamine was replaced with either a *p*-hydroxy phenol group (compound 6) or a *p*-fluoro phenyl (compound 7). The presence of the *p*-hydroxy phenol group caused a large increase in potency for all lipid kinases tested, with minimal differences in both potency and specificity for the *p*-fluoro phenyl substituent (Figure 2A).

Combining this set of information, we generated three compound 1 derivatives (compounds 8–10) that contained derivations at multiple positions of 1. All of these compounds contained a methoxy substituent off of the central phenyl, with compounds 9 and 10 containing a *p*-hydroxy phenol off of the sulfonamide and either a cyclopentyl (compound 9) or a *t*-butyl (compounds 8 and 10) group at the acetamide position off of the central thiazole. Both of the compounds containing the *p*-hydroxyl phenol were extremely potent against PI4KIII β (IC_{50} 's of 7 and 3.6 nM for compounds 9 and 10, respectively) and were >140- and >1000-fold selective over PI3K γ and >20- and >200-fold selective over PI3K δ , and they showed no inhibition of vps34 at concentrations up to 20 μ M (Figure 2B). Compound 8 was not as potent (IC_{50} of 36 nM), but it showed an excellent selectivity profile, with no inhibition of both PI3K γ and vps34 (<20% at 50 μ M) and very little inhibition of PI3K δ (<50% inhibition at 50 μ M). Compound 10 is the most potent PI4KIII β inhibitor currently reported, with very minor off-target inhibition of PI4KIII β related lipid kinases. Both compounds 9 and 10 were further characterized against a panel of six additional lipid kinases (Figure S1). Compound 9 showed weak inhibition of PI3K δ (IC_{50} –1 μ M), PI3K α (\sim 2 μ M), and PI4KIII α (\sim 2.6 μ M) and <50% inhibition at concentrations up to 20 μ M for PI4K2 α , PI4K2 β , and PI3K β . Compound 10 showed weak inhibition of

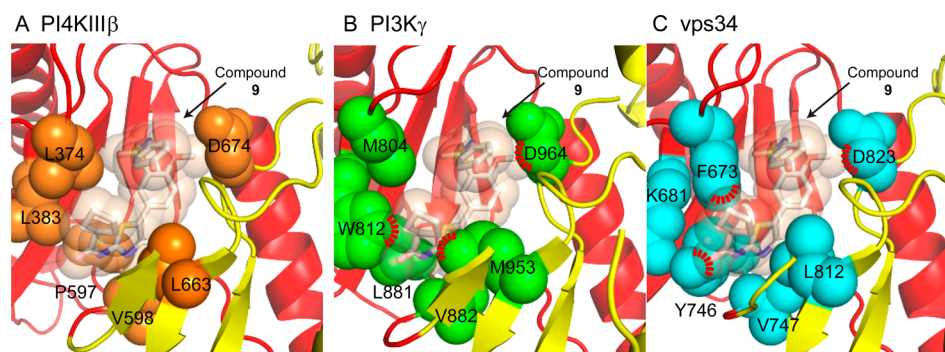


Figure 4. Structural basis for selectivity of compound **9**. (A) Structure of compound **9** bound to PI4KIII β , with selected residues colored in orange and shown as spheres. (B) Model of compound **9** in the active site of PI3K γ . The model was generated by aligning the active site of the structure of compound **9** bound to PI4KIII β to the structure of PI3K γ bound to compound **1** (PDB ID: 2CHZ). The equivalent residues shown in panel A are colored in green and shown as spheres, with steric clashes highlighted in red. (C) Model of compound **9** in the active site of vps34. The model was generated by aligning the active site of the structure of compound **9** bound to PI4KIII β to the structure of vps34 bound to compound **1** (PDB ID: 2X6). The equivalent residues shown in panel A are colored in cyan and shown as spheres, with steric clashes highlighted in red.

PI3K $C2\gamma$ (IC_{50} —1 μ M), PI3K α (\sim 10 μ M), and PI4KIII α (\sim 3 μ M), and <20% inhibition at concentrations up to 20 μ M for PI4K2 α , PI4K2 β , and PI3K β .

PI4KIII β has been shown to be a key host factor for the replication of the hepatitis C virus.^{14,21} To test the potency of the compound **1** derivative inhibitors as antivirals, we carried out viral replication assays using a luciferase reporter-linked infectious HCV clone. These results (Figures 2 and S2) generally show a trend of the most potent molecules being the most effective antivirals, with increased specificity leading to decreased toxicity. One noticeable trend in the assay was that absence of the hydroxyl-phenyl group led to a large decrease in the antiviral potency of the compounds. This may be due to differences in cell permeability caused by this group. The compounds with the best combination of antiviral efficacy and lowest toxicity were **9** and **10** (Figure S2).

Structural Basis of Specificity for PI4KIII β Inhibitors. To determine the molecular basis for the potency and specificity of these novel PI4KIII β inhibitors, we set out to crystallize them bound to PI4KIII β . We have previously crystallized a truncated construct of PI4KIII β in complex with compound **1** and the GTPase Rab11.¹⁹ This structure revealed the molecular basis of its interaction with Rab11 and also revealed the binding of compound **1** to PI4KIII β ; however, this construct crystallized only in the presence of compound **1**. To generate crystals of PI4KIII β bound to compound **9**, we used a novel crystallization construct generated through the use of a hydrogen–deuterium exchange mass spectrometry-based approach.²² This construct allowed us to generate crystals of PI4KIII β bound to GDP-loaded Rab11 in the absence of inhibitors. These crystals were used to soak compound **9** and allowed us to solve the co-crystal structure at 3.2 Å resolution. The binding mode of compound **9** was unambiguous (Figure S3). The residues mediating contacts with compound **9** are shown in Figure 3A, with the shape of the inhibitor in the active site pocket shown in Figure 3B.

Structure of PI4KIII β Bound to Compound **9.** Compound **9** forms a crescent shape that conforms to the active site of PI4KIII β . This molecule makes extensive contacts with PI4KIII β (Figure 3A). There are two putative hydrogen bonds formed between the thiazole and the acetamide of compound **9** with both the amide and carbonyl group of V598. The sulfonamide group also forms a hydrogen bond with K549. All of these hydrogen bonds are similar to those reported in the structure of **1** bound to PI4KIII β .¹⁹ Intriguingly the *p*-hydroxy group on the N-

phenol sulfonamide also makes a putative hydrogen bond with the carbonyl of G660. The presence of this *p*-hydroxyl group is important for potency because molecules lacking this group are less potent against PI4KIII β (compound **6** versus compound **7**). The presence of this hydroxyl group also increases potency for both PI3K γ and vps34, suggesting that this putative hydrogen bond is most likely conserved across all three enzymes.

The structure of compound **9** also reveals the molecular mechanism for how the acetamide and methoxy substituents mediate inhibitor selectivity over PI3K γ and vps34. Aligning the structure of PI4KIII β bound to compound **9** with structures of compound **1** bound to PI3K γ and vps34 (Figure 4A–C) reveals a number of steric clashes that explain the lack of potency of compound **9** against the PI3K family kinases. The acetamide group clashes with residues W812 and M953 in PI3K γ and residues Y746 and F673 in vps34. The methoxy group off of the central phenyl group clashes with the aspartic acid from the DFG motif in the activation loop (D964 in PI3K γ and D823 in vps34).

DISCUSSION

Phosphatidylinositol 4 kinase III β plays both key physiological and pathological roles, and the design of novel potent and selective inhibitors will be essential both in deciphering the cellular functions of this enzyme and in developing potential future therapeutic agents in diseases dependent on PI4KIII β activity. PI4KIII β mediates the replication of a variety of pathogenic RNA viruses, including members of both the *Picornaviridae* and *Flaviviridae* families of virus.¹⁰ These include viruses that pose significant threats to human health including SARS, MERS, hepatitis C, and polio. Along with this key role in mediating pathological conditions, PI4KIII β also plays key roles in a number of physiological roles including membrane trafficking,²³ lipid transport,²⁴ and cytokinesis,⁵ and the development of potent and selective molecules will be essential in deciphering the isoform-specific functions of this enzyme.

Since PI4KIII β plays an essential role in mediating viral replication for a variety of pathogenic viruses, the development of PI4KIII β inhibitors has been an attractive target for pan-antiviral agents. A number of potent PI4KIII β inhibitors have recently been discovered,^{9,12,15,21,25–28} and experiments on a variety of RNA viruses show they are potent antiviral agents. However, a complication of this work has been the toxic effects of some of these inhibitors on host function. There are conflicting results of the lethality of PI4KIII β inhibitors, with some showing lethality

in mice²⁸ and others being well-tolerated.¹⁵ Deciphering whether these effects are dependent on the inhibition of PI4KIII β or are through other off-target effects requires the generation of novel more potent and specific PI4KIII β inhibitors. A specific goal for the development of antivirals is to avoid off-target effects on both PI3K γ and PI3K δ as both of these enzymes play key roles in the immune system.²⁹

Here, we describe a set of new compound **1** derivative inhibitors that are some of the most potent and specific PI4KIII β inhibitors as yet reported. Through a detailed structure-based drug design approach, we have designed derivatives that increased potency against PI4KIII β >5-fold while increasing selectivity >1000-fold to the related lipid kinases PI3K γ and vps34. The most potent of these molecules (compound **10**) was screened over a panel of nine related lipid kinases and was >200-fold selective for PI4KIII β across all enzymes tested. Two of the most potent and selective molecules (compounds **9** and **10**) were also the most effective antiviral compounds in a cellular model of hepatitis C virus replication, with the best balance of antiviral potency and low cellular toxicity.

The structure of one of the most potent molecules bound to PI4KIII β was determined and revealed the molecular basis for the specificity of the derivative molecules. The pocket that accommodates the acetamide group of the inhibitors was found to be the most important region in mediating inhibitor selectivity, and the differences in the pocket accommodating this group in PI4KIII β compared to that in PI3K γ and vps34 explain this observation. The acetamide group mediating specificity of PI4KIII β inhibitors strongly correlates with previous studies on compounds very similar to compound **1**. Addition of a bulky substituent in a similar position to the acetamide group in compound **1** had a limited role in potency, but it greatly enhanced specificity.^{27,30} Structural and computational models of a different class of inhibitors bound to PI4KIII β suggested an important role of the pocket located near this region in mediating both potency and selectivity.²⁵ The structural details of this compound bound in the active site pocket will provide a future framework for the modification of these compounds to modify the inhibitors in a way that will enhance their pharmacokinetic properties but not lead to any decreases in their potency and specificity.

EXPERIMENTAL SECTION

Protein Expression. Truncated human PI4KIII β (121–784 Δ 249–287 Δ 408–507 S294A) (plasmid JM7) and full-length human Rab11a(Q70L) (plasmid pJB88) were expressed in BL21 C41 (DE3) cells. For Rab11a(Q70L) expression, cultures were grown to an OD₆₀₀ of 0.7 and induced with 0.5 mM IPTG for 3.5 h at 37 °C. For truncated PI4KIII β expression, cultures were induced overnight at 16 °C with 0.1 mM IPTG at an OD₆₀₀ of 0.6. Cells were harvested by centrifugation, washed with cold phosphate-buffered saline (PBS), and frozen in liquid nitrogen, and pellets were stored at –80 °C.

Protein Purification. PI4KIII β (Truncation) Purification. Cells were resuspended in 20 mM Tris-HCl, pH 8.0, 100 mM NaCl, 10 mM imidazole, 5% (v/v) glycerol, 2 mM β -mercaptoethanol, and a 1:1666 dilution of a protease inhibitor cocktail (Millipore protease inhibitor cocktail set III, animal-free) and sonicated on ice for 5 min with cycles consisting of 10 s on, 10 s off. Triton X-100 was then added to a final concentration of 0.2%, and the lysate was centrifuged for 45 min at 20 000g. The supernatant was then filtered through a 0.45 μ m filter (Celltreat Scientific Products) and was loaded onto a 5 mL HisTrap FF column (GE Healthcare) equilibrated in buffer A (20 mM Tris-HCl, pH 8.0, 100 mM NaCl, 10 mM imidazole, 5% (v/v) glycerol, 2 mM β -mercaptoethanol). The column was washed with 20 mL of buffer A, followed by 20 mL of 6% buffer B (20 mM Tris-HCl, pH 8.0, 100 mM

NaCl, 200 mM imidazole, 5% (v/v) glycerol, 2 mM β -mercaptoethanol), and it was eluted with 100% buffer B. The His affinity tag protein was cleaved overnight at 4 °C with TEV protease. The cleaved protein was then diluted to 50 mM NaCl (using 20 mM Tris-HCl, pH 8.0, 10 mM imidazole, 5% (v/v) glycerol, 2 mM β -mercaptoethanol) and was loaded onto a 5 mL HiTrap QHP column (GE Healthcare) equilibrated in buffer C (20 mM Tris-HCl, pH 8.0, 50 mM NaCl, 5% (v/v) glycerol, 2 mM β -mercaptoethanol). Protein was eluted with a gradient elution using buffer D (20 mM Tris-HCl, pH 8.0, 1.0 M NaCl, 5% (v/v) glycerol, 2 mM β -mercaptoethanol). Fractions containing the cleaved PI4KIII β were pooled and concentrated to 700 μ L in an Amicon 50K centrifugal filter (Millipore). The protein was then loaded onto a HiPrep 16/60 Sephacryl S200 column equilibrated in buffer E (20 mM HEPES, pH 7.2, 150 mM NaCl, 1 mM TCEP). The cleaved PI4KIII β was then concentrated to approximately 15 mg/mL in an Amicon 50K centrifugal filter (Millipore), and aliquots were frozen in liquid nitrogen and stored at –80 °C.

Rab11a(Q70L) Purification. Cells were resuspended in 20 mM Tris-HCl, pH 8.0, 100 mM NaCl, 5% (v/v) glycerol, 2 mM β -mercaptoethanol, and a 1:1666 dilution of a protease inhibitor cocktail (Millipore protease inhibitor cocktail set III, animal-free). Cells were sonicated and centrifuged as described for the truncated PI4KIII β . The supernatant was filtered through a 0.45 μ m filter (Celltreat Scientific Products) and incubated for 1 h with 4 mL of glutathione Sepharose 4B beads (GE Healthcare) equilibrated in buffer F (20 mM Tris-HCl, pH 8.0, 100 mM NaCl, 5% (v/v) glycerol, 2 mM β -mercaptoethanol) followed by a 3 \times 15 mL wash in buffer F. The GST tag was cleaved overnight on the beads with TEV protease. Anion-exchange chromatography was performed as outlined above for the truncated PI4KIII β . Cleaved Rab11a(Q70L) was then concentrated to between 5 and 15 mg/mL and nucleotide loaded by adding EDTA to 10 mM followed by 1 U of phosphatase (phosphatase, alkaline-agarose from calf intestine; Sigma P0762-100UN) per milligram of protein. Proteins were then incubated for 1.5 h. The phosphatase was removed using a 0.2 μ m spin filter (Millipore); the flow-through was collected, and a 10-fold molar excess of GDP was added followed by MgCl₂ to a final concentration of 20 mM. Proteins were incubated for 30 min. Gel filtration was performed with cleaved GDP-loaded Rab11a(Q70L) as described above for the truncated PI4KIII β .

Crystallography. Crystals of PI4KIII β (final concentration 7.4 mg/mL) with Rab11a-GDP (final concentration 4.5 mg/mL) were obtained in 15% (w/v) PEG-4000, 100 mM sodium citrate, pH 5.6, 200 mM ammonium sulfate (protein/precipitant ratio of 3:1). Refinement plates were set by gridding PEG-4000, ammonium sulfate, and glycerol. Optimized crystals were obtained by seeding using the Hampton Research seed bead kit according to the manufacturer's instructions using a reservoir solution of 14.8% (w/v) PEG-4000, 100 mM sodium citrate, pH 5.6, 250 mM ammonium sulfate. The best crystals were obtained in 13–15% (w/v) PEG-4000, 100 mM sodium citrate, pH 5.6, 250 mM ammonium sulfate, and 2% glycerol with a 1/1000 or 1/10000 seed solution dilution, a Rab11a-GDP final concentration of 4.51 mg/mL, and a PI4KIII β final concentration of 7.38 mg/mL. Crystals were frozen in liquid nitrogen using a 15% PEG-4000 (w/v), 100 mM sodium citrate, pH 5.6, 250 mM ammonium sulfate, and 25% (v/v) glycerol cryo solution.

Inhibitor soaks were performed by incubating crystals with 0.5 μ L of 10 μ M inhibitor stocks in cryo buffer (15% PEG-4000 (w/v), 250 mM ammonium sulfate, 100 mM sodium citrate, pH 5.6, 25% glycerol (v/v)) for 30 min, followed by a 30 min incubation with 0.5 μ L of 100 μ M inhibitor stock in cryo buffer and a final 30 min incubation in 1 mM inhibitor stock in cryo buffer. Before the final addition, 1 μ L was removed from the crystal drop and 1 μ L of the 1 mM inhibitor in cryo buffer was added.

Diffraction data were collected at 100 K at beamline 08ID-1 of the Canadian Macromolecular Crystallography Facility (Canadian Light Source, CLS). Data were integrated using iMosflm 7.1.1³¹ and scaled with AIMLESS.³² Phases were initially obtained by molecular replacement (MR) using Phaser,³³ with the structure of PI4KIII β bound to compound **1** and Rab11 (PDB ID: 4D0L) used as the search model. The final model of PI4KIII β bound to compound **9** in complex

with Rab11 was built using iterative model building in COOT³⁴ and refinement using Phenix^{35,36} to $R_{\text{work}} = 23.87$ and $R_{\text{free}} = 26.79$. The binding mode of compound **9** was unambiguous, and ligand geometry was generated using the elbow subset of Phenix.³⁷ Full crystallographic statistics are shown in Table 1.

Table 1. Data Collection and Refinement Statistics^a

data collection	PI4K–Rab11–GDP–compound 9
wavelength (Å)	0.9797
space group	$P2_12_12_1$
unit cell	(48.9 103.5 188.9), (90 90 90)
total reflections	67660 (6441)
unique reflections	16316 (1611)
multiplicity	4.1 (4.0)
completeness (%)	98.63 (99.44)
mean $I/\sigma(I)$	8.93 (2.11)
Wilson B-factor	82.35
R_{merge}	0.1092 (0.7019)
R_{meas}	0.1249
CC1/2	0.993 (0.375)
CC*	0.998 (0.738)
Refinement	
resolution range (Å)	47.34–3.2 (3.31–3.2)
reflections used for R_{free}	5%
R_{work}	23.3 (32.9)
R_{free}	26.6 (38.0)
no. of non-hydrogen atoms	5041
macromolecules	4970
ligands	71
water	0
protein residues	619
RMS (bonds)	0.003
RMS (angles)	0.61
Ramachandran favored (%)	96
Ramachandran outliers (%)	0.17
clashscore	21.91
average B-factor	99
macromolecules	98.8
ligands	109

^aStatistics for the highest-resolution shell are shown in parentheses.

Biochemical Assays. Lipid kinase assays were preformed using recombinant enzyme, phosphoinositides purchased from Avanti Polar Lipids, and $\gamma^{32}\text{P}$ -ATP (PerkinElmer cat. no. BLU502A001MC) in a membrane capture assay described previously.³⁸ Each inhibitor was diluted into 10% DMSO and kinase assay buffer. Upon completion of the reaction, 4 μL was spotted onto 0.2 μm nitrocellulose (Bio-Rad cat. no. 162-0112). The membrane was dried for 5 min under a heat lamp followed by 1 \times 30 s and 6 \times 5 min washes in 1 M NaCl/1% phosphoric acid. The membrane was dried for 20 min under a heat lamp followed by overnight exposure to a phosphor screen, and phosphorimaging followed on a Typhoon 9500. Intensities were quantified using SPOT.³⁸ Specifications for each enzyme follow.

PI4KIII β . Recombinant enzyme was purchased from Life Technologies (cat. no. PV5277, lot no. 943589E). *L*- α -Phosphatidylinositol (PI, cat. no. 840024P) and DOPS:DOPC lipids (cat. no. 790595P) were sonicated in water to generate 1 mg/mL PI:DOPS:DOPC. The reaction was setup as follows: (1) kinase assay buffer, PI:DOPS:DOPC, BSA, and PI4KIII β were combined in a total volume of 10 μL (2.5 \times solution); (2) 5 μL of inhibitor solution was added (5 \times solution) and incubated with the enzyme mixture for 15 min; and (3) 10 μL of cold ATP and $\gamma^{32}\text{P}$ -ATP was added (2.5 \times solution) to initiate the reaction, which ran for 30 min. Final conditions were as follows: 20 mM Bis-Tris Propane, pH 7.5, 10 mM MgCl₂, 0.075 mM Triton X-100, 0.5 mM EGTA, 1 mM DTT,

100 μM PI, 500 ng/ μL BSA, 2.5 nM PI4KIII β , 2% DMSO, 10 μM ATP, and 1 μCi $\gamma^{32}\text{P}$ -ATP.

PI3K γ . Recombinant enzyme was purchased from Life Technologies (cat. no. PV4786, lot no. 1638926A). *L*- α -Phosphatidylinositol-4,5-bisphosphate (PIP₂, cat. no. 840046P) and DOPS:DOPC lipids (cat. no. 790595P) were sonicated in water to generate 1 mg/mL PIP₂:DOPS:DOPC. The reaction was setup as follows (1) kinase assay buffer, PIP₂:DOPS:DOPC, BSA, and PI3K γ were combined in a total volume of 10 μL (2.5 \times solution); (2) 5 μL of inhibitor solution was added (5 \times solution) and incubated with the enzyme mixture for 15 min; and (3) 10 μL of cold ATP and $\gamma^{32}\text{P}$ -ATP was added (2.5 \times solution) to initiate the reaction, which ran for 15 min. Final conditions were as follows: 50 mM HEPES, pH 7.5, 100 mM NaCl, 0.03% CHAPS, 10 mM MgCl₂, 1 mM EGTA, 2 mM DTT, 5 nM PI3K γ , 80 μM PIP₂, 500 ng/ μL BSA, 2% DMSO, 10 μM ATP, and 1 μCi $\gamma^{32}\text{P}$ -ATP.

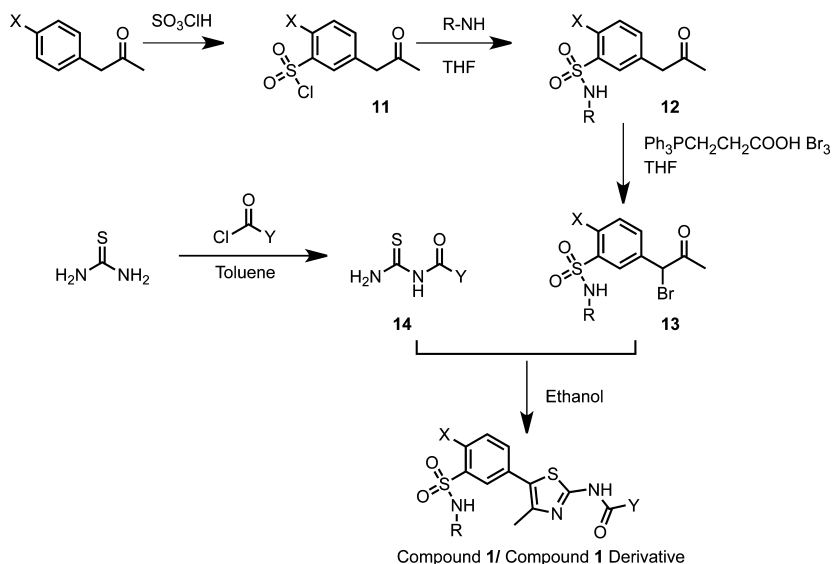
PI3K δ . Recombinant enzyme was purchased from Life Technologies (cat. no. PV6451, lot no. 1763224). *L*- α -Phosphatidylinositol-4,5-bisphosphate (PIP₂, cat. no. 840046P) and DOPS:DOPC lipids (cat. no. 790595P) were sonicated in water to generate 1 mg/mL PIP₂:DOPS:DOPC. The reaction was setup as follows: (1) kinase assay buffer, PIP₂:DOPS:DOPC, BSA, and PI3K δ were combined in a total volume of 10 μL (2.5 \times solution); (2) 5 μL of inhibitor solution was added (5 \times solution) and incubated with the enzyme mixture for 15 min; and (3) 10 μL of cold ATP and $\gamma^{32}\text{P}$ -ATP was added (2.5 \times solution) to initiate the reaction, which ran for 20 min. Final conditions were as follows: 50 mM HEPES, pH 7.5, 100 mM NaCl, 0.03% CHAPS, 10 mM MgCl₂, 1 mM EGTA, 2 mM DTT, 2.5 nM PI3K δ , 80 μM PIP₂, 500 ng/ μL BSA, 2% DMSO, 10 μM ATP, and 2.5 μCi $\gamma^{32}\text{P}$ -ATP.

vps34. Recombinant enzyme was purchased from Life Technologies (cat. no. PV5126, lot no. 1555138A). *L*- α -Phosphatidylinositol (PI, cat. no. 840024P) and DOPS:DOPC lipids (cat. no. 790595P) were sonicated in water to generate 1 mg/mL PI:DOPS:DOPC. The reaction was setup as follows: (1) kinase assay buffer, PI:DOPS:DOPC, BSA, and vps34 were combined in a total volume of 10 μL (2.5 \times solution); (2) 5 μL of inhibitor solution was added (5 \times solution) and incubated with the enzyme mixture for 15 min; and (3) 10 μL of cold ATP and $\gamma^{32}\text{P}$ -ATP was added (2.5 \times solution) to initiate the reaction, which ran for 1 h. Final conditions were as follows: 50 mM HEPES, pH 7.5, 0.1% CHAPS, 2 mM MnCl₂, 1 mM EGTA, 2 mM DTT, 10 nM vps34, 100 μM PI, 500 ng/ μL BSA, 2% DMSO, 10 μM ATP, and 2.5 μCi $\gamma^{32}\text{P}$ -ATP.

PI4KIII α . Recombinant enzyme was purchased from EMD Millipore (cat. no. 14-908, lot no. D9KN031N-B). *L*- α -Phosphatidylinositol (PI, cat. no. 840024P) and DOPS:DOPC lipids (cat. no. 790595P) were sonicated in water to generate 1 mg/mL PI:DOPS:DOPC. The reaction was setup as follows: (1) kinase assay buffer, PI:DOPS:DOPC, BSA, and PI4KIII α were combined in a total volume of 10 μL (2.5 \times solution); (2) 5 μL of inhibitor solution was added (5 \times solution) and incubated with the enzyme mixture for 15 min; and (3) 10 μL of cold ATP and $\gamma^{32}\text{P}$ -ATP was added (2.5 \times solution) to initiate the reaction, which ran for 25 min. Final conditions were as follows: 20 mM Bis-Tris Propane, pH 7.5, 10 mM MgCl₂, 0.075 mM Triton X-100, 0.5 mM EGTA, 1 mM DTT, 100 μM PI, 500 ng/ μL BSA, 1.2 nM PI4KIII α , 2% DMSO, 10 μM ATP, and 2 μCi $\gamma^{32}\text{P}$ -ATP.

PI4KII α . PI4KII α was cloned from DNASU plasmid HsCD00003332.^{39,40} Recombinant enzyme was obtained through FLAG immunoprecipitation of FLAG-PI4KII α transfected into HEK293T cells (10 μg of FLAG-PI4KII α transfected with Life Technologies Lipofectamine and Plus Reagent to a 15 cm dish of HEK293Ts and 75 μL elution with FLAG peptide). *L*- α -Phosphatidylinositol (PI, cat. no. 840024P) and DOPS:DOPC lipids (cat. no. 790595P) were sonicated in water to generate 1 mg/mL PI:DOPS:DOPC. The reaction was setup as follows: (1) kinase assay buffer, PI:DOPS:DOPC, BSA, and PI4KII α were combined in a total volume of 10 μL (2.5 \times solution); (2) 5 μL of inhibitor solution was added (5 \times solution) and incubated with the enzyme mixture for 15 min; and (3) 10 μL of cold ATP and $\gamma^{32}\text{P}$ -ATP was added (2.5 \times solution) to initiate the reaction, which ran for 25 min. Final conditions were as follows: 20 mM Bis-Tris Propane, pH 7.5, 10 mM MgCl₂, 0.075 mM Triton X-100, 0.5 mM EGTA, 1 mM DTT, 100 μM PI, 500 ng/ μL BSA, 2.9 μL of PI4KII α , 2% DMSO, 10 μM ATP, and 2 μCi $\gamma^{32}\text{P}$ -ATP.

Scheme 1. Synthesis of Compound 1 and Derivatives



PI4KII β . PI4KII β was cloned from DNASU plasmid HsCD00001592.^{39,40} Recombinant enzyme was obtained through FLAG immunoprecipitation of FLAG-PI4KII β transfected into HEK293T cells (10 μ g of FLAG-PI4KII β transfected with Life Technologies Lipofectamine and Plus Reagent to a 15 cm dish of HEK293Ts and 75 μ L elution with FLAG peptide). L- α -Phosphatidylinositol (PI, cat. no. 840024P) and DOPS:DOPC lipids (cat. no. 790595P) were sonicated in water to generate 1 mg/mL PI:DOPS:DOPC. The reaction was setup as follows: (1) kinase assay buffer, PI:DOPS:DOPC, BSA, and PI4KII β were combined in a total volume of 10 μ L (2.5 \times solution); (2) 5 μ L of inhibitor solution was added (5 \times solution) and incubated with the enzyme mixture for 15 min; and (3) 10 μ L of cold ATP and γ ³²P-ATP was added (2.5 \times solution) to initiate the reaction, which ran for 25 min. Final conditions were as follows: 20 mM Bis-Tris Propane, pH 7.5, 10 mM MgCl₂, 0.075 mM Triton X-100, 0.5 mM EGTA, 1 mM DTT, 100 μ M PI, 500 ng/ μ L BSA, 2 μ L of PI4KII β , 2% DMSO, 10 μ M ATP, and 2 μ Ci γ ³²P-ATP.

PI3K α . Recombinant enzyme was purchased from EMD Millipore (cat. no. 14-602, lot no. 2150294-A). L- α -Phosphatidylinositol-4,5-bisphosphate (PIP₂, cat. no. 840046P) and DOPS:DOPC lipids (cat. no. 790595P) were sonicated in water to generate 1 mg/mL PIP₂:DOPS:DOPC. The reaction was setup as follows: (1) kinase assay buffer, PIP₂:DOPS:DOPC, BSA, and PI3K α were combined in a total volume of 10 μ L (2.5 \times solution); (2) 5 μ L of inhibitor solution was added (5 \times solution) and incubated with the enzyme mixture for 15 min; and (3) 10 μ L of cold ATP and γ ³²P-ATP was added (2.5 \times solution) to initiate the reaction, which ran for 15 min. Final conditions were as follows: 50 mM HEPES, pH 7.5, 100 mM NaCl, 0.03% CHAPS, 10 mM MgCl₂, 1 mM EGTA, 2 mM DTT, 3.3 nM PI3K α , 80 μ M PIP₂, 500 ng/ μ L BSA, 2% DMSO, 10 μ M ATP, and 2 μ Ci γ ³²P-ATP.

PI3K β . Recombinant enzyme was purchased from SignalChem (cat. no. P28-10H-10, lot no. F-532-3). L- α -Phosphatidylinositol-4,5-bisphosphate (PIP₂, cat. no. 840046P) and DOPS:DOPC lipids (cat. no. 790595P) were sonicated in water to generate 1 mg/mL PIP₂:DOPS:DOPC. The reaction was setup as follows: (1) kinase assay buffer, PIP₂:DOPS:DOPC, BSA, and PI3K β were combined in a total volume of 10 μ L (2.5 \times solution); (2) 5 μ L of inhibitor solution was added (5 \times solution) and incubated with the enzyme mixture for 15 min; and (3) 10 μ L of cold ATP and γ ³²P-ATP was added (2.5 \times solution) to initiate the reaction, which ran for 15 min. Final conditions were as follows: 50 mM HEPES, pH 7.5, 100 mM NaCl, 0.03% CHAPS, 10 mM MgCl₂, 1 mM EGTA, 2 mM DTT, 0.6 nM PI3K β , 80 μ M PIP₂, 500 ng/ μ L BSA, 2% DMSO, 10 μ M ATP, and 2 μ Ci γ ³²P-ATP.

PI3K2 γ . Recombinant enzyme was purchased from EMD Millipore (cat. no. 14-910, lot no. 2023057-A). L- α -Phosphatidylinositol (PI, cat. no. 840024P) and DOPS:DOPC lipids (cat. no. 790595P) were

sonicated in water to generate 1 mg/mL PI:DOPS:DOPC. The reaction was setup as follows: (1) kinase assay buffer, PI:DOPS:DOPC, BSA, and PI3K2 γ were combined in a total volume of 10 μ L (2.5 \times solution); (2) 5 μ L of inhibitor solution was added (5 \times solution) and incubated with the enzyme mixture for 15 min; and (3) 10 μ L of cold ATP and γ ³²P-ATP was added (2.5 \times solution) to initiate the reaction, which ran for 15 min. Final conditions were as follows: 50 mM HEPES, pH 7.5, 100 mM NaCl, 0.03% CHAPS, 10 mM MgCl₂, 1 mM EGTA, 2 mM DTT, 1 nM PI3K2 γ , 100 μ M PI, 500 ng/ μ L BSA, 2% DMSO, 10 μ M ATP, and 2 μ Ci γ ³²P-ATP.

Organic Synthesis. Materials obtained commercially were reagent grade and were used without further purification. ¹H NMR spectra were recorded on a Varian 400 spectrometer at 400 MHz. High-resolution electron impact mass spectra were recorded on a Thermo Fisher Exactive EMR and Thermo Fisher LTQ Orbitrap Velos at the University of California–San Francisco Center for Mass Spectrometry. Reactions were monitored by thin-layer chromatography using Merck silica gel 60 F₂₅₄ glass plates (0.25 mm thick). Flash chromatography was conducted with Grace Reveleris flash cartridges with 40 μ m silica on an Agilent 971-FP. All RP-HPLC were performed with a Waters 2545 binary gradient module equipped with an XBridge prep C18 column using H₂O + 0.1% formic acid and CH₃CN + 0.1% formic acid (5–95% gradient) while monitoring at 254 nm. All final compounds were >95% pure, as measured by liquid chromatography mass spectrometry (LCMS). Full compound characterization details are presented in the [Supporting Information](#).

Synthesis of compound 1 and derivatives was conducted similarly to methods described previously¹⁷ and is shown in [Scheme 1](#). To commercially available acetophenone was added chlorosulfuric acid (11 equiv) dropwise in an ice bath, and the reaction was heated at 40 $^{\circ}$ C for 2 h. The reaction was stopped by dropwise transfer to ice water. The aqueous phase was extracted 3 \times with ethyl acetate, and the combined organic was dried with sodium sulfate, filtered, and concentrated *in vacuo* to give a brown oil, the crude, corresponding to sulfonyl chloride 11. The sulfonyl chloride was dissolved in THF (1.5 M), the appropriate amino alcohol (4.5 equiv) was added, and the reaction was allowed to stir overnight at room temperature. The reaction was concentrated *in vacuo*, water was added, and the aqueous phase was extracted 3 \times with ethyl acetate. The combined organic phase was concentrated, and intermediate 12 was purified using silica gel flash chromatography (2–10% methanol in dichloromethane). If pure intermediate was not obtained, then the intermediate was subjected to a second purification by reverse-phase HPLC using acetonitrile/water/0.1% formic acid as the solvent system.

Intermediate 12 was dissolved in THF (1.5 M). (2-Carboxyethyl)-triphenylphosphonium bromide was dissolved in THF (1 M), and

intermediate **12** was added to the bromide solution dropwise at room temperature. The reaction was allowed to proceed 1 h at room temperature, the solvent was removed *in vacuo*, and the product was purified by silica gel flash chromatography (0–10% methanol in dichloromethane) to yield intermediate **13**.

To ethanol-recrystallized thiourea in dry toluene (0.5 M) was added the appropriate acyl chloride, and the reaction was heated to reflux for 18 h. Toluene was removed *in vacuo*, and the reaction was diluted in ethyl acetate and filtered. The organic layer was washed 2× with water and brine, dried with sodium sulfate, and reduced *in vacuo*. The resulting acetylthiourea **14** was purified by silica gel flash chromatography (25–100% ethyl acetate in hexanes).

Intermediate **13** was dissolved in ethanol (0.17 M), and appropriate acetylthiourea **14** was added at room temperature. The reaction was heated to reflux for 30 min and then cooled to room temperature, and compound **1** or a compound **1** derivative (compounds **2–10**) was purified by silica gel chromatography (0–10% methanol in dichloromethane), which, if necessary, was followed by reverse-phase HPLC using acetonitrile/water/0.1% formic acid as the solvent system.

Gaussia Luciferase-Based HCV Reporter Virus and Stable Cell Line of Huh7.5 Containing Infectious HCV Reporter Virus. A fully infectious HCVcc genotype 2a reporter virus encoding *Gaussia* luciferase between p7 and NS2 similar to that used by Maurkian et al.⁴¹ was generated to monitor HCV replication quantitatively. Briefly, *Gaussia* luciferase gene with an in-frame foot and mouth disease virus autoproteolytic 2A peptide sequence was inserted between HCV p7 and NS2 of a J6/JFH1 infectious HCV clone,⁴² resulting in the fully infectious HCVcc reporter virus J6/JFH1-GLuc (p7-NS2-GLucFM2A). After Huh7.5 cells were infected with the *Gaussia* luciferase-based HCV reporter virus, the cells were maintained for 3 days and then passaged every 4 days for 20 passages. A stable cell line with consistent *Gaussia* luciferase secretion was established.

HCV2a Antiviral Assay. Huh7.5 cells stably infected with J6/JFH1-GLuc were maintained and passaged in DMEM (Mediatech, Manassas, VA) supplemented with 10% FBS (Omega Scientific, Tazana, CA), 2 mM glutamine (Mediatech, Manassas, VA), nonessential amino acids (Mediatech, Manassas, VA), 100 IU/mL penicillin (Mediatech, Manassas, VA), and 100 mg/mL streptomycin (Mediatech, Manassas, VA) and were cultured in a 37 °C incubator with 5% CO₂ and 95% relative humidity.

Ten thousand cells were plated in 96-well plates (E&K Scientific Products, Santa Clara, CA) and supplemented with serially diluted compounds 1 h after plating. After 3 days of incubation, viability was tested using the Presto Blue cell viability reagent (Life Technologies Corporation, Grand Island, NY) per the manufacturer's protocol, and replication was measured by determining the *Gaussia* luciferase activity in the supernatant using the luciferase reagent (Promega Corporation, Madison, WI) according to the manufacturer's protocol.

Viability and luminescence were read using a plate reader (Infinite 1000, Tecan Systems, San Jose, CA). Values were imported into Prism (GraphPad Software, La Jolla, CA) for graphing and calculations of IC₅₀ and CC₅₀ values.

■ ASSOCIATED CONTENT

Supporting Information

The Supporting Information is available free of charge on the ACS Publications website at DOI: 10.1021/acs.jmedchem.5b01311.

Compound characterization; inhibitor assays of compounds **9** and **10** across a panel of lipid kinases; antiviral efficacy and toxicity of selected inhibitors; binding of compound **9** in the active site pocket of PI4KIIIβ (PDF) SMILES strings, IC₅₀ data, and CC₅₀ data for **1–10** (CSV)

Accession Codes

The structure factors and PDB coordinates of PI4K bound to compound **9** have been deposited at the protein databank (PDB) with the coordinates 5EUQ.

■ AUTHOR INFORMATION

Corresponding Authors

*(K.M.S.) E-mail: kevan.shokat@ucsf.edu. Tel.: 1-415-514-0472.

*(J.E.B.) E-mail: jeburke@uvic.ca. Tel.: 1-250-721-8732.

Present Address

[†](M.A.G.) Department of Medicine, Veterans Administration Medical Center, Bronx, New York 10468, United States.

Author Contributions

[#]F.U.R. and M.L.F. contributed equally to this work.

Notes

The authors declare the following competing financial interest(s): The compounds reported here are the subject of a provisional patent application by UCSF, on which F.U.R., B.T., and K.M.S. are co-inventors.

■ ACKNOWLEDGMENTS

J.E.B. wishes to thank CIHR for support (CIHR new investigator grant and CIHR open operating grant FRN 142393). K.M.S. and J.S.G. wish to thank NIH for support (R01 AI099245 and U19 AI109622). M.A.G. wishes to thank NIH for support (K08 AI097322). We thank the staff at the Canadian Light Source (CLS) CMC-FID beamline, where diffraction data were collected. The CLS is supported by the Natural Sciences and Engineering Research Council of Canada, the National Research Council Canada, the Canadian Institutes of Health Research, the Province of Saskatchewan, Western Economic Diversification Canada, and the University of Saskatchewan. High-resolution mass spectrometry was provided by the Bio-Organic Biomedical Mass Spectrometry Resource at UCSF (A.L. Burlingame, Director), supported by the Biomedical Technology Research Centers program of the NIH National Institute of General Medical Sciences, NIH NIGMS 8P41GM103481 and NIH 1S10OD016229, and the Howard Hughes Medical Institute. F.U.R. wishes to thank NSF for support (Grant No. 1144247).

■ ABBREVIATIONS USED

PI4K, phosphatidylinositol 4 kinase; PI3K, phosphoinositide 3 kinase; PI4P, phosphatidylinositol 4-phosphate; PIP₂, phosphatidylinositol 4,5-bisphosphate; PIP₃, phosphatidylinositol 3,4,5-trisphosphate

■ REFERENCES

- (1) Balla, T. Phosphoinositides: Tiny Lipids with Giant Impact on Cell Regulation. *Physiol. Rev.* **2013**, *93*, 1019–1137.
- (2) Dornan, G. L.; McPhail, J. A.; Burke, J. E. Type III Phosphatidylinositol 4 Kinases: Structure, Function, Regulation, Signalling and Involvement in Disease. *Biochem. Soc. Trans.* **2016**, *44*, 260–266.
- (3) Tan, J.; Brill, J. A. Cinderella Story: PI4P Goes From Precursor to Key Signaling Molecule. *Crit. Rev. Biochem. Mol. Biol.* **2014**, *49*, 33–58.
- (4) Tóth, B.; Balla, A.; Ma, H.; Knight, Z. A.; Shokat, K. M.; Balla, T. Phosphatidylinositol 4-Kinase IIIβ Regulates the Transport of Ceramide Between the Endoplasmic Reticulum and Golgi. *J. Biol. Chem.* **2006**, *281*, 36369–36377.
- (5) Polevoy, G.; Wei, H.-C.; Wong, R.; Szentpetery, Z.; Kim, Y. J.; Goldbach, P.; Steinbach, S. K.; Balla, T.; Brill, J. A. Dual Roles for the Drosophila PI 4-Kinase Four Wheel Drive in Localizing Rab11 During Cytokinesis. *J. Cell Biol.* **2009**, *187*, 847–858.
- (6) Sridhar, S.; Patel, B.; Aphkhasava, D.; Macian, F.; Santambrogio, L.; Shields, D.; Cuervo, A. M. The Lipid Kinase PI4KIIIβ Preserves Lysosomal Identity. *EMBO J.* **2012**, *32*, 324–339.

- (7) Jean, S.; Kiger, A. A. Coordination Between RAB GTPase and Phosphoinositide Regulation and Functions. *Nat. Rev. Mol. Cell Biol.* **2012**, *13*, 463–470.
- (8) Hsu, N.-Y.; Ilnytska, O.; Belov, G.; Santiana, M.; Chen, Y.-H.; Takvorian, P. M.; Pau, C.; van der Schaar, H.; Kaushik-Basu, N.; Balla, T.; Cameron, C. E.; Ehrenfeld, E.; van Kuppeveld, F. J. M.; Altan-Bonnet, N. Viral Reorganization of the Secretory Pathway Generates Distinct Organelles for RNA Replication. *Cell* **2010**, *141*, 799–811.
- (9) McNamara, C. W.; Lee, M. C. S.; Lim, C. S.; Lim, S. H.; Roland, J.; Nagle, A.; Simon, O.; Yeung, B. K. S.; Chatterjee, A. K.; McCormack, S. L.; Manary, M. J.; Zeeman, A.-M.; Dechering, K. J.; Kumar, T. R. S.; Henrich, P. P.; Gagaring, K.; Ibanez, M.; Kato, N.; Kuhlen, K. L.; Fischli, C.; Rottmann, M.; Plouffe, D. M.; Bursulaya, B.; Meister, S.; Rameh, L.; Trappe, J.; Haasen, D.; Timmerman, M.; Sauerwein, R. W.; Suwanarusk, R.; Russell, B.; Renia, L.; Nosten, F.; Tully, D. C.; Kocken, C. H. M.; Glynn, R. J.; Bodenreider, C.; Fidock, D. A.; Diagona, T. T.; Wenzel, E. A. Targeting Plasmodium PI(4)K to Eliminate Malaria. *Nature* **2013**, *504*, 248–253.
- (10) Altan-Bonnet, N.; Balla, T. Phosphatidylinositol 4-Kinases: Hostages Harnessed to Build Panviral Replication Platforms. *Trends Biochem. Sci.* **2012**, *37*, 293–302.
- (11) Mello, C.; Aguayo, E.; Rodriguez, M.; Lee, G.; Jordan, R.; Cihlar, T.; Birkus, G. Multiple Classes of Antiviral Agents Exhibit in Vitro Activity Against Human Rhinovirus Type C. *Antimicrob. Agents Chemother.* **2014**, *58*, 1546–1555.
- (12) van der Schaar, H. M.; van der Linden, L.; Lanke, K. H. W.; Strating, J. R. P. M.; Pürstinger, G.; de Vries, E.; de Haan, C. A. M.; Neyts, J.; van Kuppeveld, F. J. M. Coxsackievirus Mutants That Can Bypass Host Factor PI4KIII β and the Need for High Levels of PI4P Lipids for Replication. *Cell Res.* **2012**, *22*, 1576–1592.
- (13) Greninger, A. L.; Knudsen, G. M.; Betegon, M.; Burlingame, A. L.; DeRisi, J. L. The 3A Protein From Multiple Picornaviruses Utilizes the Golgi Adaptor Protein ACBD3 to Recruit PI4KIII β . *J. Virol.* **2012**, *86*, 3605–3616.
- (14) Borawski, J.; Troke, P.; Puyang, X.; Gibaja, V.; Zhao, S.; Mickanin, C.; Leighton-Davies, J.; Wilson, C. J.; Myer, V.; Cornellataracido, L.; Baryza, J.; Tallarico, J.; Joberty, G.; Bantscheff, M.; Schirle, M.; Bouwmeester, T.; Mathy, J. E.; Lin, K.; Compton, T.; Labow, M.; Wiedmann, B.; Gaither, L. A. Class III Phosphatidylinositol 4-Kinase Alpha and Beta Are Novel Host Factor Regulators of Hepatitis C Virus Replication. *J. Virol.* **2009**, *83*, 10058–10074.
- (15) van der Schaar, H. M.; Leyssen, P.; Thibaut, H. J.; de Palma, A.; van der Linden, L.; Lanke, K. H. W.; Lacroix, C.; Verbeken, E.; Conrath, K.; Macleod, A. M.; Mitchell, D. R.; Palmer, N. J.; van de Poël, H.; Andrews, M.; Neyts, J.; van Kuppeveld, F. J. M. A Novel, Broad-Spectrum Inhibitor of Enterovirus Replication That Targets Host Cell Factor Phosphatidylinositol 4-Kinase III β . *Antimicrob. Agents Chemother.* **2013**, *57*, 4971–4981.
- (16) Arita, M.; Kojima, H.; Nagano, T.; Okabe, T.; Wakita, T.; Shimizu, H. Phosphatidylinositol 4-Kinase III Beta Is a Target of Enviroxime-Like Compounds for Antipoliiovirus Activity. *J. Virol.* **2011**, *85*, 2364–2372.
- (17) Knight, Z.; Gonzalez, B.; Feldman, M.; Zunder, E.; Goldenberg, D.; Williams, O.; Loewith, R.; Stokoe, D.; Balla, A.; Toth, B.; Balla, T.; Weiss, W.; Williams, R.; Shokat, K. A Pharmacological Map of the PI3-K Family Defines a Role for P110alpha in Insulin Signaling. *Cell* **2006**, *125*, 733–747.
- (18) Balla, A.; Kim, Y. J.; Várnai, P.; Szentpetery, Z.; Knight, Z.; Shokat, K. M.; Balla, T. Maintenance of Hormone-Sensitive Phosphoinositide Pools in the Plasma Membrane Requires Phosphatidylinositol 4-Kinase IIIalpha. *Mol. Biol. Cell* **2007**, *19*, 711–721.
- (19) Burke, J. E.; Inglis, A. J.; Perisic, O.; Masson, G. R.; McLaughlin, S. H.; Rutaganira, F.; Shokat, K. M.; Williams, R. L. Structures of PI4KIII β Complexes Show Simultaneous Recruitment of Rab11 and Its Effectors. *Science* **2014**, *344*, 1035–1038.
- (20) Miller, S.; Tavshanjian, B.; Oleksy, A.; Perisic, O.; Houseman, B.; Shokat, K.; Williams, R. Shaping Development of Autophagy Inhibitors with the Structure of the Lipid Kinase Vps34. *Science* **2010**, *327*, 1638–1642.
- (21) Lamarche, M. J.; Borawski, J.; Bose, A.; Capacci-Daniel, C.; Colvin, R.; Dennehy, M.; Ding, J.; Dobler, M.; Drumm, J.; Gaither, L. A.; Gao, J.; Jiang, X.; Lin, K.; McKeever, U.; Puyang, X.; Raman, P.; Thohan, S.; Tommasi, R.; Wagner, K.; Xiong, X.; Zabawa, T.; Zhu, S.; Wiedmann, B. Anti-Hepatitis C Virus Activity and Toxicity of Type III Phosphatidylinositol-4-Kinase Beta Inhibitors. *Antimicrob. Agents Chemother.* **2012**, *56*, 5149–5156.
- (22) Rutaganira, F. U.; Shokat, K. M.; Williams, R. L.; Burke, J. E. Using Hydrogen Deuterium Exchange Mass Spectrometry to Engineer Optimized Constructs for Crystallization of Protein Complexes: Case Study of PI4KIII β with Rab11. *Protein Sci.* **2016**, DOI: 10.1002/pro.2879.
- (23) Jovic, M.; Kean, M. J.; Szentpetery, Z.; Polevoy, G.; Gingras, A.-C.; Brill, J. A.; Balla, T. Two Phosphatidylinositol 4-Kinases Control Lysosomal Delivery of the Gaucher Disease Enzyme, B-Glucocerebrosidase. *Mol. Biol. Cell* **2012**, *23*, 1533–1545.
- (24) D'Angelo, G.; Vicinanza, M.; Wilson, C.; De Matteis, M. A. Phosphoinositides in Golgi Complex Function. *Subcell. Biochem.* **2012**, *59*, 255–270.
- (25) Mejdrová, I.; Chalupská, D.; Kögler, M.; Šála, M.; Plačková, P.; Baumlová, A.; Hřebabeký, H.; Procházková, E.; Dejmejk, M.; Guillon, R.; Strunin, D.; Weber, J.; Lee, G.; Birkus, G.; Mertlíková-Kaiserová, H.; Boura, E.; Nencka, R. Highly Selective Phosphatidylinositol 4-Kinase III β Inhibitors and Structural Insight Into Their Mode of Action. *J. Med. Chem.* **2015**, *58*, 3767–3793.
- (26) Arita, M.; Philipov, S.; Galabov, A. S. Phosphatidylinositol 4-Kinase III Beta Is the Target of Oxoglucine and Pachypodol (Ro 09–0179) for Their Anti-Poliiovirus Activities, and Locates at Upstream of the Target Step of Brefeldin a. *Microbiol. Immunol.* **2015**, *59*, 338–347.
- (27) Waring, M. J.; Andrews, D. M.; Faulder, P. F.; Flemington, V.; McKelvie, J. C.; Maman, S.; Preston, M.; Raubo, P.; Robb, G. R.; Roberts, K.; Rowlinson, R.; Smith, J. M.; Swarbrick, M. E.; Treinies, I.; Winter, J. J. G.; Wood, R. J. Potent, Selective Small Molecule Inhibitors of Type III Phosphatidylinositol-4-Kinase A- but Not B-Inhibit the Phosphatidylinositol Signaling Cascade and Cancer Cell Proliferation. *Chem. Commun. (Cambridge, U. K.)* **2014**, *50*, 5388–5390.
- (28) Spickler, C.; Lippens, J.; Labege, M.-K.; Desmeules, S.; Bellavance, É.; Garneau, M.; Guo, T.; Hucke, O.; Leyssen, P.; Neyts, J.; Vaillancourt, F. H.; Décor, A.; O'Meara, J.; Franti, M.; Gauthier, A. Phosphatidylinositol 4-Kinase III Beta Is Essential for Replication of Human Rhinovirus and Its Inhibition Causes a Lethal Phenotype in Vivo. *Antimicrob. Agents Chemother.* **2013**, *57*, 3358–3368.
- (29) Okkenhaug, K. Signaling by the Phosphoinositide 3-Kinase Family in Immune Cells. *Annu. Rev. Immunol.* **2013**, *31*, 675–704.
- (30) Keaney, E. P.; Connolly, M.; Dobler, M.; Karki, R.; Honda, A.; Sokup, S.; Karur, S.; Britt, S.; Patnaik, A.; Raman, P.; Hamann, L. G.; Wiedmann, B.; LaMarche, M. J. 2-Alkylloxazoles as Potent and Selective PI4KIII β Inhibitors Demonstrating Inhibition of HCV Replication. *Bioorg. Med. Chem. Lett.* **2014**, *24*, 3714–3718.
- (31) Batty, T. G. G.; Kontogiannis, L.; Johnson, O.; Powell, H. R.; Leslie, A. G. W. iMOSFLM: a New Graphical Interface for Diffraction-Image Processing with MOSFLM. *Acta Crystallogr., Sect. D: Biol. Crystallogr.* **2011**, *67*, 271–281.
- (32) Evans, P. R.; Murshudov, G. N. How Good Are My Data and What Is the Resolution? *Acta Crystallogr., Sect. D: Biol. Crystallogr.* **2013**, *69*, 1204–1214.
- (33) McCoy, A. J.; Grosse-Kunstleve, R. W.; Adams, P. D.; Winn, M. D.; Storoni, L. C.; Read, R. J. Phaser Crystallographic Software. *J. Appl. Crystallogr.* **2007**, *40*, 658–674.
- (34) Emsley, P.; Lohkamp, B.; Scott, W. G.; Cowtan, K. Features and Development of Coot. *Acta Crystallogr., Sect. D: Biol. Crystallogr.* **2010**, *66*, 486–501.
- (35) Adams, P. D.; Afonine, P. V.; Bunkóczi, G.; Chen, V. B.; Echols, N.; Headd, J. J.; Hung, L.-W.; Jain, S.; Kapral, G. J.; Grosse-Kunstleve, R. W.; McCoy, A. J.; Moriarty, N. W.; Oeffner, R. D.; Read, R. J.; Richardson, D. C.; Richardson, J. S.; Terwilliger, T. C.; Zwart, P. H. The Phenix Software for Automated Determination of Macromolecular Structures. *Methods* **2011**, *55*, 94–106.

(36) Afonine, P. V.; Grosse-Kunstleve, R. W.; Echols, N.; Headd, J. J.; Moriarty, N. W.; Mustyakimov, M.; Terwilliger, T. C.; Urzhumtsev, A.; Zwart, P. H.; Adams, P. D. Towards Automated Crystallographic Structure Refinement with Phenix.Refine. *Acta Crystallogr., Sect. D: Biol. Crystallogr.* **2012**, *68*, 352–367.

(37) Moriarty, N. W.; Grosse-Kunstleve, R. W.; Adams, P. D. Electronic Ligand Builder and Optimization Workbench (eLBOW): a Tool for Ligand Coordinate and Restraint Generation. *Acta Crystallogr., Sect. D: Biol. Crystallogr.* **2009**, *65*, 1074–1080.

(38) Knight, Z.; Feldman, M.; Balla, A.; Balla, T.; Shokat, K. A Membrane Capture Assay for Lipid Kinase Activity. *Nat. Protoc.* **2007**, *2*, 2459–2466.

(39) Seiler, C. Y.; Park, J. G.; Sharma, A.; Hunter, P.; Surapaneni, P.; Sedillo, C.; Field, J.; Algar, R.; Price, A.; Steel, J.; Throop, A.; Fiocco, M.; Labaer, J. DNASU Plasmid and PSI:Biological-Materials Repositories: Resources to Accelerate Biological Research. *Nucleic Acids Res.* **2014**, *42*, D1253–D1260.

(40) Park, J.; Hu, Y.; Murthy, T. V. S.; Vannberg, F.; Shen, B.; Rolfs, A.; Hutti, J. E.; Cantley, L. C.; Labaer, J.; Harlow, E.; Brizuela, L. Building a Human Kinase Gene Repository: Bioinformatics, Molecular Cloning, and Functional Validation. *Proc. Natl. Acad. Sci. U. S. A.* **2005**, *102*, 8114–8119.

(41) Marukian, S.; Jones, C. T.; Andrus, L.; Evans, M. J.; Ritola, K. D.; Charles, E. D.; Rice, C. M.; Dustin, L. B. Cell Culture-Produced Hepatitis C Virus Does Not Infect Peripheral Blood Mononuclear Cells. *Hepatology* **2008**, *48*, 1843–1850.

(42) Cho, N.-J.; Lee, C.; Pang, P. S.; Pham, E. A.; Fram, B.; Nguyen, K.; Xiong, A.; Sklan, E. H.; Elazar, M.; Koytak, E. S.; Kersten, C.; Kanazawa, K. K.; Frank, C. W.; Glenn, J. S. Phosphatidylinositol 4,5-Bisphosphate Is an HCV NS5A Ligand and Mediates Replication of the Viral Genome. *Gastroenterology* **2015**, *148*, 616–625.

(43) Laskowski, R. A.; Swindells, M. B. LigPlot+: Multiple Ligand-Protein Interaction Diagrams for Drug Discovery. *J. Chem. Inf. Model.* **2011**, *51*, 2778–2786.